Characterization of nanoscale silver particles in glasses by temperature-dependent EXAFS spectroscopy

2000 J. Phys.: Condens. Matter 12 4775

(http://iopscience.iop.org/0953-8984/12/22/310)

J. Phys.: Condens. Matter **12** (2000) 4775–4789. Printed in the UK PII: S0953-8984(00)11283-4

Characterization of nanoscale silver particles in glasses by temperature-dependent EXAFS spectroscopy

M Dubiel†, S Brunsch† and L Tröger‡

† University of Halle-Wittenberg, Department of Physics, Friedemann-Bach-Platz 6, 06108 Halle, Germany

‡ Hamburger Synchrotronstrahlungslabor, Deutsches Elektronensynchrotron, D-22603 Hamburg, Germany

Received 24 January 2000

Abstract. The structural parameters of nanoscale silver particles embedded in a silicate glass matrix have been determined by temperature-dependent EXAFS spectroscopy at the Ag K edge for two particle sizes of 2.5 and 6 nm. EXAFS measurements allowed us to probe both the oxygen environment of silver ions separated within the glass matrix and the structure of precipitated silver particles. The lattice parameter of the Ag particles showed an unusual dilatation of the silver structure that is a result of the glass cooling process. Furthermore, an increase was found of static and dynamic Debye–Waller factors as well as of the thermal expansion coefficient compared with bulk Ag material. The experiments demonstrate that the behaviour of metal particles incorporated into a glass matrix reflects size effects of nanoscaled particles and the influence of the surrounding matrix.

1. Introduction

Nanoscale metal particles embedded in a dielectric matrix, like Ag, Au or Cu in silicate glasses, have attracted much interest as materials for optical devices and other applications of non-linear parameters (see, e.g., [1, 2]). It is well known that the electronic as well as the atomic structure is considerably changed as the size increases from clusters to small particles and, at last, to bulk material through which manifold interesting properties are developed. We can observe, e.g. a melting point depression, a lattice contraction or an increasing ionization potential of particles in the nanometre size range as compared with that of bulk metal [3, 4]. This behaviour can be explained by the increased number of surface atoms for clusters and small particles, respectively. By incorporating the particles into a surrounding matrix, usually, a variation of such effects is expected due to the interaction of metal atoms across the particle–matrix interface. It has been demonstrated that interactions at the interface can even reverse the sign of these variations in comparison to non-embedded particles. As examples, it was observed that the melting temperature of In particles embedded in an Al matrix is higher than that of bulk material [5]. Also, the lattice parameter of silver particles with a size of 1 nm prepared by the inert-gas aggregation technique showed a dilatation measured by high resolution electron microscopy [6]. EXAFS experiments on thiol-capped CdS nanoparticles show an expansion of the mean Cd–S distance due to steric interactions between the ligands [7]. These examples demonstrate a number of unexpected results concerning the nanoscale particles as well as diverse explanation of these effects. Thus,

0953-8984/00/224775+15$30.00

it seems to be important to reflect upon the preparation procedure and the thermal history in each case with respect to the interaction between small particles and a support or a surrounding matrix, respectively.

Silver particles in soda-lime glasses, which will be considered in the present work, can be incorporated into a silicate glass matrix by various routes. Here, Ag/Na ion exchange and subsequent thermal annealing was used. In order to study the effects of particle size and preparation method, it is necessary to determine the atomic structure of nanoscale particles and of the particle–glass interface with high accuracy. These results should reveal the relationship between particle configuration and macroscopic behaviour of the glass. A few methods are available to characterize the structure of nanoscale particles. There are spectroscopic techniques, which are directly sensitive to the structure of nanoscale particles like diffraction experiments (x-ray, neutrons, electrons), high resolution electron microscopy (HREM) and extended x-ray absorption fine structure (EXAFS) measurements. Structural characterization by x-ray diffraction requires a crystalline order and a particle size of some nanometres, otherwise the broadening of diffraction peaks does not allows structural parameters to be determined. The imaging of crystalline lattice planes of individual particles can be achieved by electron microscopy up to a size of particles of approximately 1 nm. The experiments are carried out usually at room temperature. Compared with that the EXAFS spectroscopy reveals interatomic distances with increased accuracy from both crystalline lattices and disordered structures without any limitations concerning particle sizes. However, the structural data derived from such experiments include pair correlations from atoms at the surface as well as at the interior of the particle. Furthermore, it has to be mentioned that conventional absorption experiments, e.g. at the Ag K edge, yield averaged information on the whole number of silver species within the sample, i.e. of isolated silver ions, clusters and small particles. These effects have to be considered in order to interpret the EXAFS parameters like bond lengths or coordination numbers. There are many articles which discuss the evaluation of EXAFS data of nanoscale particles. Recently, the evaluation of temperature-dependent EXAFS experiments including anharmonic distributions of bond lengths showed averaged lattice parameters as well as the Debye temperature and the thermal expansion coefficient of small particles and bulk materials [8–15].

The purpose of the present work is to investigate silver particles in ion-exchanged soda-lime glasses containing increased amounts of iron oxide, so called green glasses. Previous experiments on soda-lime glasses containing small amounts of polyvalent ions, i.e. less than 0.1% of Fe or other, demonstrated the formation of silver particles, e.g. by optical spectroscopy or electron microscopy [16]. Nevertheless, the amount of silver ions exceeds by far silver incorporated in crystalline particles. Consequently, the contribution of Ag–Ag correlations to the EXAFS oscillations is small which does not allow an accurate study of the structure of nanoscale particles [17, 18]. Therefore, the preparation procedure was varied in such a way that the Ag–Ag contribution should dominate Ag–O correlations within the radial distribution function of EXAFS data. The temperature dependence of the Ag–Ag separation will be evaluated on the basis of an anharmonic Einstein model [8, 13, 14] by the ratio method combined with the cumulant expansion technique up to the third- or fourth-order term. The EXAFS data like Ag–Ag coordination number, average distance, Debye–Waller factor and high-order cumulants characterize the structure and size of particles. The comparison of these parameters with crystalline Ag bulk material should enlighten the influence of quantum size effects, the interaction between the particles and the surrounding matrix across the glass–particle interface as well as thermal effects induced by the preparation procedure. The results will be discussed in connection with experiments by high resolution electron microscopy.

2. Experiment

2.1. Sample preparation

The precipitation of small Ag particles has been investigated on soda-lime glasses (Flachglas AG, Germany) containing increased amounts of iron oxide, so-called green glasses. The composition of float glasses (in weight%) is 71.87% SiO_2, 13.30% Na_2O, 8.69% CaO, 4.15% MgO, 0.59% Al_2O_3, 0.31% K_2O, 0.01% BaO, 0.079% TiO_2, 0.148% SO_3 and 0.865% Fe_2O_3. The Sn containing surface was removed by polishing in order to exclude additional reduction of silver ions within the surface layer by Sn^{2+} ions. The portion of Fe^{2+} to the total iron content amounts to 26%, i.e. there is sufficient reducing agent available to enable Ag precipitation [19].

By an ion exchange at 330 °C in nitrate melts (0.05% $AgNO_3$/99.95% $NaNO_3$) silver ions were introduced into the glass structure exchanging silver for sodium. A thickness of glass plates of 0.30 mm and an extended exchange period of 307 hours were chosen to achieve a nearly homogeneous silver distribution across the sample. The exchange ratio Ag/(Ag+Na) was less than 10% that allows the silver ions to be reduced by Fe^{2+}. The nanoscale Ag particles were formed as a result of reduction and aggregation processes due to subsequent thermal treatment around the glass transformation temperature.

2.2. EXAFS spectroscopy

EXAFS spectra at the Ag K edge (25514 eV) were collected at the positron storage ring DORIS III at beam line X1 (RÖMO II) of HASYLAB in Hamburg, Germany. An Si(311) double-crystal monochromator was used with an energy resolution of $\Delta E/E \cong 2 \times 10^{-4}$. Harmonic rejection was achieved by detuning the monochromator crystals by 50%. Absorption experiments were performed in transmission mode between 10 and 300 K using a liquid helium vapour flow cryostat. The x-ray intensity was measured with ionization chambers. Silver foils and Ag_2O were used as crystalline standards for data analysis. The optimum thickness of the samples was attained by superimposing the appropriate number of glass plates.

3. Data evaluation and thermal expansion

The program package UWXAFS [20, 21] was used for normalization and background removal by a cubic spline fit. The extracted EXAFS oscillations $\chi(T, k)$ that result from backscattering atoms surrounding the absorber atom are given by [22–24]

$$\chi(T,k) = \sum_i (N_i/kr_i^2(T))S_i^2(k)F_i(k)\exp(-2\sigma_i^2(T)k^2 + 2C_{4,i}(T)k^4/3)\exp(-2r_i(T)/\lambda) \times \sin(2kr_i(T) + \varphi_i(T,k) - 4\sigma_i^2 k/r_i[1 + r_i/\lambda] - 4C_{3,i}(T)k^3/3) \quad (1)$$

where k is the wave number of the photoelectrons ejected; N_i is the number of neighbours within the ith coordination sphere at distance $r_i(T)$. The $F_i(k)$ describe the characteristic backscattering amplitudes of the neighbouring atoms. The damping of the amplitude is induced by many-body effects described by S_i^2, the Debye–Waller factor, $\sigma_i^2(T)$, and the limited mean free path, λ, of the ejected photoelectrons. The scattering phase shift is characterized by $\varphi_i(k)$. Anharmonicity effects of radial distribution of bond lengths, e.g. due to surface atoms or thermal expansion effects, are considered by third-order and fourth-order cumulants, C_3 and C_4, respectively. Of course, C_3 and C_4 can be neglected for symmetric distribution of bond distances. $\chi(T, k)$ of each coordination sphere can be separated into two contributions,

i.e. the amplitude and the phase function:

$$\chi(T,k) = A(T,k)\sin\Phi(T,k). \tag{2}$$

The cumulant coefficients can be determined [22, 24, 25] by the logarithmic plot of amplitudes of glasses, A, and reference Ag foil, A_0, versus k^2

$$\ln[A(T,k)/A_0(T,k)] = \ln[Nr_0^2(T)/N_0r^2(T)] - 2(\sigma^2(T) - \sigma_0^2(T))k^2 + 2C_4(T)k^4/3 \tag{3}$$

and by the corresponding phase difference divided by $2k$ versus k^2

$$[\Phi(T,k) - \Phi_0(T,k)]/2k = r(T) - r_0(T) - [\sigma^2(T) - \sigma_0^2(T)][2/r(T) + 2/\lambda] - 2C_3(T)k^2/3. \tag{4}$$

This equation is valid under the assumption that the cumulant coefficients, C_3 and C_4, of the reference sample can be neglected. By this ratio method the parameters C_3, C_4 and σ^2 were calculated for all glass samples at different temperatures on the basis of Ag foil data measured at 10 K. The resulting parameters were used as starting points for fitting procedure. The theoretical amplitude and phase functions calculated by FEFF7 based on the curved wave theory [20, 26] were used for Ag–Ag and for Ag–O correlations. The threshold energy, E_0, of the Ag K edge was determined by the first derivative of the Ag foil spectra which were always measured at room temperature at the same time. The edge shift for the glass samples was estimated by fitting for each sample at the lowest experimental temperature (10 K/50 K). For higher temperatures these values were fixed.

The normalized spectra $\chi(k)$ were weighted by k^2 and Fourier transformed using a Hanning window function. The weighting by k^2 was chosen in order to well separate Ag–O and Ag–Ag correlations. The coordination numbers of the different shells were fitted in real space between 1.5 and 4.05 Å at 10/50 K for each sample on the basis of theoretical amplitude and phase functions by FEFF7. At higher temperatures these values were fixed. The anharmonicity parameters, C_3 and C_4, obtained by the ratio method were used as starting points of fitting procedure and variations were only allowed in small ranges.

A quantity of interest in composite materials containing small particles is the thermal expansion of the particles. Usually, such materials are prepared by various thermal treatments. Thus, the thermal expansion coefficient of each component influences the behaviour of the composite. Similar to the structural effects mentioned above the coefficient depends strongly on the particle size up to a size of approximately 10 nm because of drastic structural changes in the transformation range between clusters and the bulk material. The EXAFS data should allow to estimate the thermal expansion by the precise calculation of the change of $r(T)$, e.g. by equation (4). Due to the accuracy of determination of $r(T)$ from EXAFS phase, the temperature-dependent variation of Debye–Waller factor within the EXAFS phase term as well as possible effects concerning small particles [14]; however, this method currently does not show the required precision. Therefore, an anharmonic Einstein model and thermodynamic perturbation theory will be used instead to describe thermal expansion behaviour [12, 13, 27]. Within this model, the linear expansion parameter, α, can be calculated from the temperature dependence of only higher cumulants, σ^2 and C_3, assuming an anharmonic potential:

$$\alpha = \frac{c_3}{rT\sigma^2}\frac{3z(1+z)\ln(1/z)}{(1-z)(1+10z+z^2)}$$

with $z = \exp(-\Theta_E/T)$, where

$$\Theta_E = \frac{\hbar\omega}{k_B} \qquad \text{and} \qquad \sigma^2 = \frac{\hbar}{2\mu\omega}\frac{(1+z)}{(1-z)}. \tag{5}$$

4. Results

The normalized EXAFS spectra of Ag foil, glass I and II are shown in figures 1 and 2. The temperature-dependent spectra of Ag foil as a reference structure were evaluated on the basis of Ag K edge spectra of silver foil measured at 10 K. This low-temperature spectrum was fitted by means of theoretical phase and amplitude function of FEFF 7 that yield an Ag–Ag coordination number of 12 as expected for crystalline fcc lattices. Corresponding Fourier transforms of the glass samples and the silver foil at 50 K are represented in figure 3 together with their fits. The fundamental shape of the Fourier transforms of the glasses is very similar to that of silver foil. These spectra indicate the existence of crystalline silver particles incorporated in the glass matrix that is confirmed by electron microscopy (see figures 4 and 5 and [28]). The averaged size determined by transmission electron microscopy was found to be 6 nm after an annealing at 600/580 °C (glass I) and 2.5 nm after an annealing at 410/480 °C (glass II), respectively.

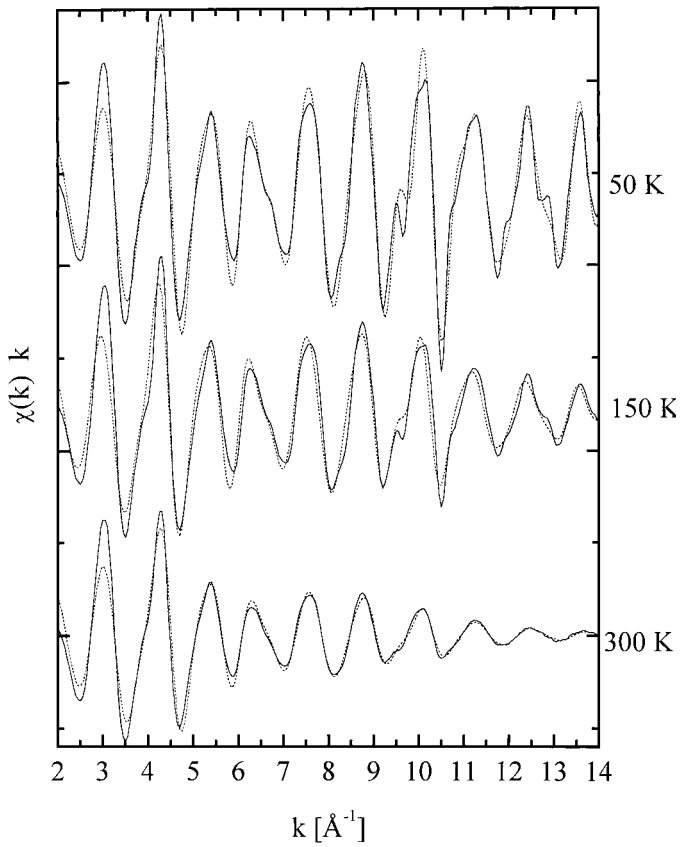

Figure 1. EXAFS oscillations weighted by k of Ag foil in dependence on the temperature. Further experiments were performed at 75, 100, 200 and 250 K. The dashed lines represent the result of fitting the Fourier transforms by UWXAFS.

Additionally, a small contribution of Ag–O environment is observed for glass samples. This part of the spectra is assigned to isolated silver ions, which are not incorporated in silver particles. The fit procedure includes this oxygen environment of silver ions that is well known

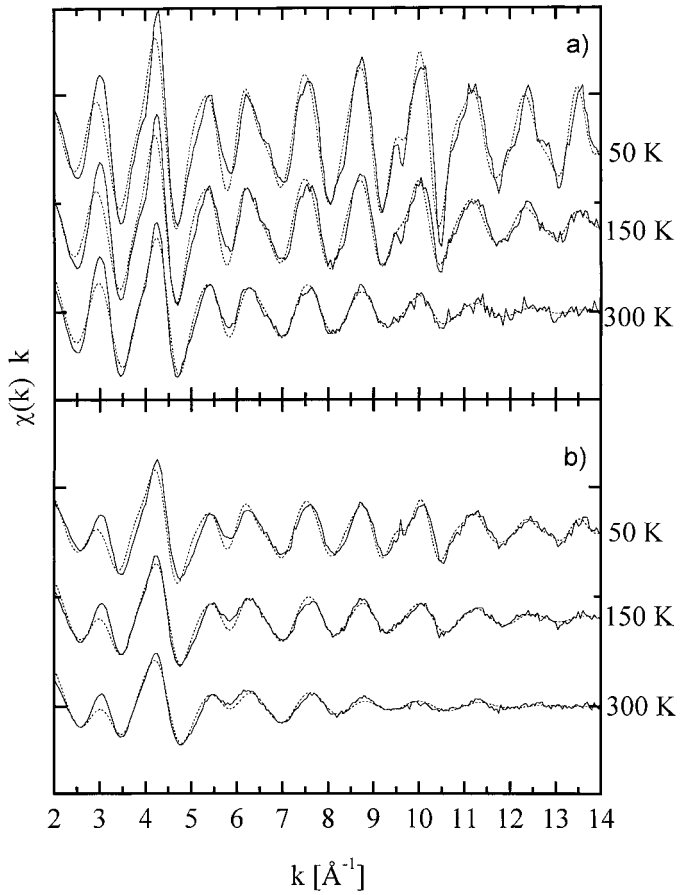

Figure 2. EXAFS data of (a) glass I containing Ag particles of 6 nm in size and of (b) glass II containing Ag particles of 2.5 nm. The results of the fitting procedure are shown by the dashed lines.

from ion-exchanged samples [17]. In the case of Ag–Ag correlations, four neighbouring spheres were considered, but only the parameters of the first two spheres were fitted. Excellent agreement between fitted and experimental data is shown in figure 3. The sum of the squared deviations of the experimental functions from the fitted ones is in the order of 0.01.

Figures 6–8 illustrate the temperature dependence of the fit parameters r, σ^2 and C_3 obtained for the first Ag–Ag sphere. The accuracy of parameters is $\Delta r = 0.003$ Å, $\Delta\sigma^2 = 0,001$ Å^2 and $\Delta C_3 = 2 \times 10^{-5}$ Å^3, respectively. The Ag–Ag distances of the silver particles and the silver foil increase over the whole temperature range with increasing temperature as expected due to thermal expansion. The difference between the EXAFS data of the silver foil and the thermodynamical values of the Ag fcc structure, which are represented in figure 6 in addition, will be discussed later. The mean-square relative displacement values, σ^2, of the particles in glass I closely resemble the one of the silver foil, but, in glass II σ^2 is significantly larger. The Einstein temperature can be estimated by a fit of the temperature-dependent Debye–Waller factor using equation (5). The fits are shown in figure 7 and the parameters are summarized in table 1. The Einstein temperature of Ag foil is 165 K that is in agreement with thermodynamical data [29] as well as with earlier EXAFS experiments [8].

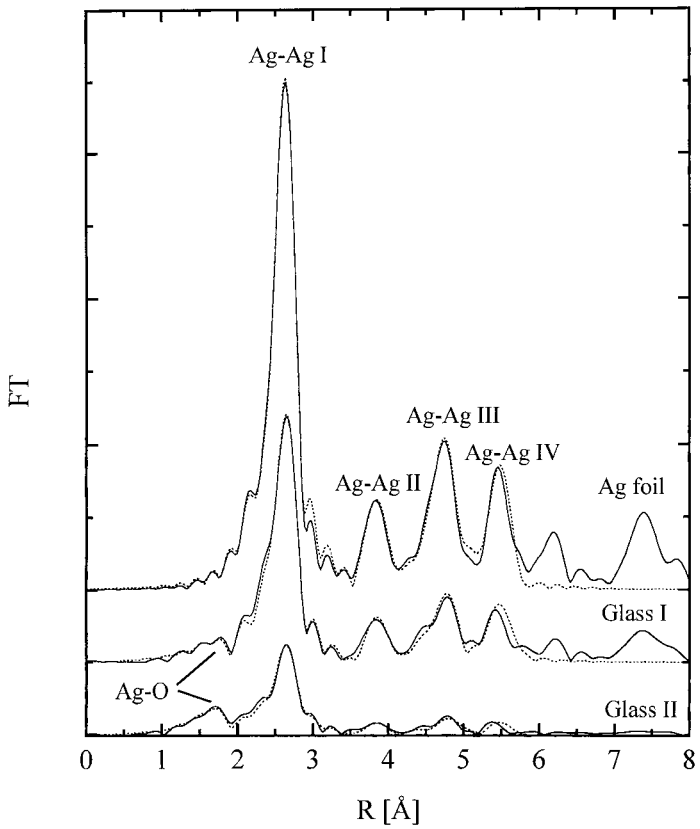

Figure 3. Fourier transformation of EXAFS oscillations measured at 50 K and the corresponding results of fitting FT(R) (dashed lines) using UWXAFS.

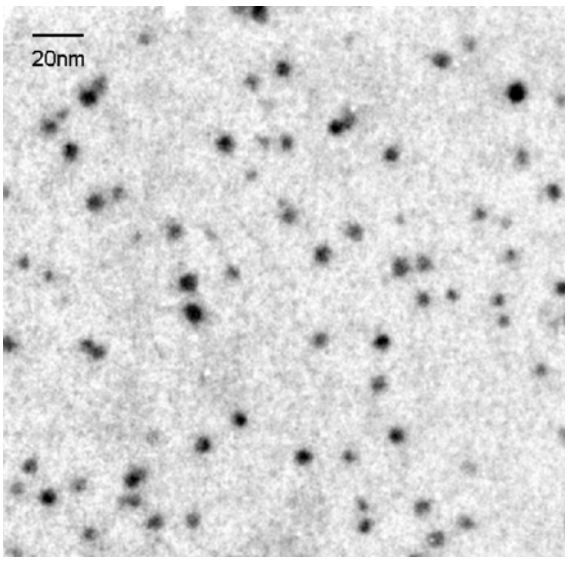

Figure 4. Ag particles in glass formed upon thermal treatment at 480 °C. The penetration depth of silver into the glass sample, i.e. the distance of this position from the glass surface, is 75 μm.

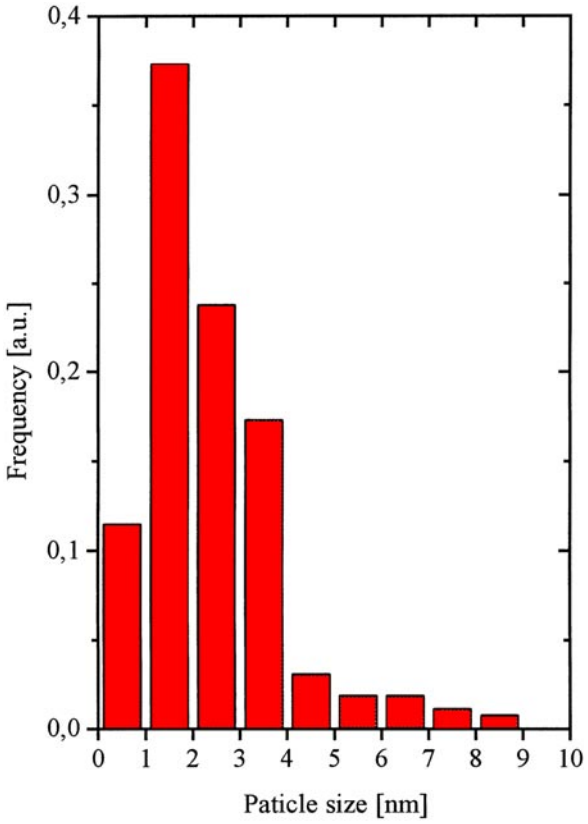

Figure 5. Size distribution of silver particles resulting from particles at various penetration depths after annealing at 480 °C. With this the mean diameter was calculated to be 2.5 nm.

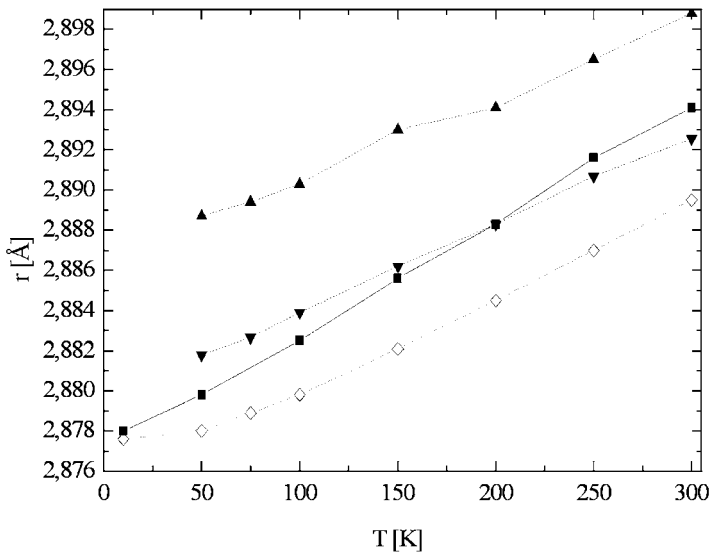

Figure 6. Comparison of Ag–Ag distances of particles (▼2.5 nm, ▲6 nm) and silver foil (■) with thermodynamical data (◇) of fcc bulk material [30].

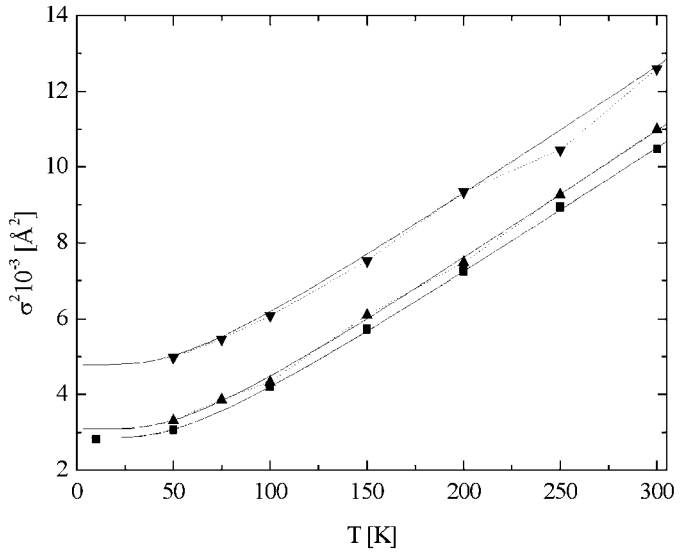

Figure 7. Mean-square relative displacement calculated by fitting experimental data using the Einstein model (dotted line). The symbols for the experimental data are the same as in figure 4.

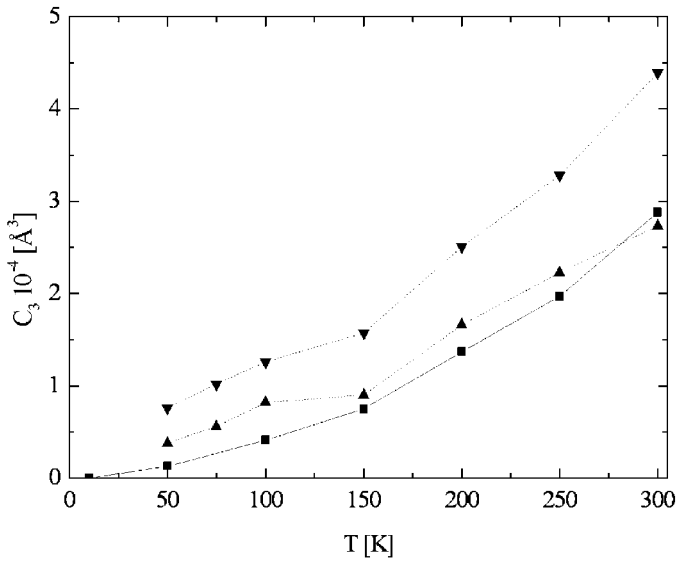

Figure 8. The values of the third cumulant, C_3, calculated for the first Ag–Ag coordination sphere. The symbols for the experimental data are the same as in figure 4.

The third cumulants, C_3, were calculated on the assumption that this value vanishes for the crystalline Ag lattice at the lowest temperature. It was found that the fourth cumulant, C_4, could always be neglected. To calculate the thermal expansion coefficient by equation (5) the Einstein temperature, the Debye–Waller factor and the third cumulant were used. As shown in table 1, averaged values for the thermal expansion coefficient were calculated in the temperature range between 200 and 250 K, which are the most reliable data in a temperature

Table 1. Parameters obtained from EXAFS data analysis for Ag foil and for small particles embedded in glass matrix. Structural data are given for the Ag–Ag pair correlations of metallic particles and for Ag–O bonds reflecting silver ions isolated within the glass network. The estimated error in the Ag–Ag coordination number is 10%, in the Einstein temperature 2 K, in the thermal expansion coefficient 0.3×10^{-5} K^{-1}, in the Ag–O distance 0.003 Å and in the Ag–O coordination number 20%, respectively.

	Size of Ag particles [nm]	Ag–Ag coordination number	Einstein temperature	Thermal expansion coefficient [10^{-5} K^{-1}]	Ag–O distance [Å]	Ag–O coordination number
Ag foil		12	165 ([29] 165)	1.68 ([30] 1.80)		
Glass I	6	6.5	161	1.78	2.128	0.5
Glass II	2.5	3.2	161	2.04	2.145	0.8

range with nearly constant thermal expansion. The resulting coefficient of Ag foil that is shown in table 1 corresponds well within the accuracy of data with thermodynamical data as well as with previous EXAFS investigations [9, 30]. These results allow us to use EXAFS spectroscopy to investigate the thermal expansion of silver particles in glasses. The data of the Ag–O coordination that was detected in the glass samples are included in table 1. The Debye–Waller factor was of the order of 0.0025 Å^2; however, this fit parameter shows a reduced accuracy due to the small portion of Ag–O correlations to the total spectrum.

5. Discussion

5.1. Separation of Ag–O and Ag–Ag correlations

Electron microscopical observations demonstrated an average size of particles of 6 nm for glass I and of 2.5 nm for glass II, respectively. The silver particles are formed by reduction, nucleation and aggregation processes subsequent to the incorporation of silver ions during the ion exchange. The thermal treatment at elevated temperatures, which causes the precipitation of crystalline particles, leads to a defined ratio between isolated and aggregated silver species. This is clearly evident by the Ag–O portion of the EXAFS spectrum of glasses as well as by the reduced Ag–Ag coordination number. The averaged oxygen coordination number in table 1 is less than one and the Ag–O distance is nearby 0.215 nm that was already found at the beginning of the ion exchange process without any formation of particles [31]. The reduced Ag–O coordination number which is usually nearby two for silver ions in sodium silicate glasses [31, 32] results from Ag atoms without any oxygen neighbours, i.e. atoms situated within the silver particles. Therefore, these data are consistent with the previous supposition that a typical environment of ionic silver in a silicate glasses exists independent on concentration effects or aggregation phenomena.

In table 1 is shown a decreased Ag–Ag coordination number of silver containing glasses compared with crystalline Ag fcc lattice. In a first approximation, the value of the Ag–Ag coordination number is a result of the mixture of two types of Ag environment as mentioned for Ag–O coordination. There are the silver ions isolated within the glass matrix and the silver atoms incorporated into silver particles. Such a configuration was also assumed for irradiated Ag-doped soda-lime glasses [33]. The average coordination number of silver within ideally spherical nanoscaled particles would be reduced to 9.6 for a particle size of 2.5 nm and to 11.0 for a particle size of 6 nm [34], respectively, as a result of the well defined number of surface

atoms. The Ag–Ag coordination number of isolated silver ions was assumed to be zero. These assumptions yield a portion of silver ions $Ag^+/(Ag^+ + Ag^0)$ in glass I of 48% and in glass II of 67%, respectively. On the basis of Ag–O coordination number the same procedure leads to a percentage of 25% (glass I) and 40% (glass II). These data demonstrate the existence of a considerable amount of isolated silver species. The differences between the two calculations are caused by the simplified model. It is expected that additionally a number of charged or non-charged clusters with sizes less than 1 nm are formed which cannot be detected by electron microscopy. The formation of an oxide layer at the surface of particles [35] is unlikely because of the low tendency of oxidization of silver and because of electron microscopical observations that could confirm pure crystalline fcc lattices without layer structures. Thus, the main contributions to the Ag EXAFS spectrum of glass samples can be explained by the two different environments of silver within (i) the glass network and within (ii) the Ag particles. In the following, the Debye–Waller factor, the third cumulant and the bond length of the first Ag–Ag coordination sphere of silver particles are discussed in more detail.

5.2. Debye–Waller factor

It is obvious from figure 7 that the Ag–Ag Debye–Waller factor of glass I with a particle size of 6 nm exhibits a similar behaviour as the bulk material. The fit by equation (5) yields an Einstein temperature of 161 K (see table 1) that reflects a small increase of disorder with respect to the bulk value. However, particles of a size of 6 nm, i.e. particles containing approximately 4000 atoms with a proportion of surface atoms of 25%, incorporated into a glass matrix do not differ distinctly from bulk material. For smaller particles, the influence of surface atoms will be evident in spite of the surrounding glass matrix. Glass II contains silver particles with an average size of 2.5 nm. These particles are formed by 309 silver atoms from which 50% are at the surface of the particle, i.e. at the interface between glass and particle. Here, the Debye–Waller factor that represents the mean-square relative displacement of the interatomic distances can be subdivided into a temperature-dependent part, σ_{dyn}, and a temperature-independent part, σ_{static}, which can be described by equation (5). The separation of both parts yields an Einstein temperature of 161 K and a static Debye–Waller factor higher by 0.002 $Å^2$ in glass II. The static term reflects in the main the disorder of the silver atoms within the interface between crystalline particle and disordered glass network that is, particularly, evident for 2.5 nm particles because of the increased proportion of surface atoms of 50%. Electron microscopy showed spherical particles predominantly without any crystalline surface planes like (111) or (100) [28]. This supports the EXAFS data. The temperature dependence of σ_{dyn} characterized by the Einstein temperature reflects the different vibration behaviour of surface atoms compared with volume atoms. The value of 161 K is the same as for the larger particles of glass I. It is to be expected that both particle size and interface structure influence the Einstein temperature. These data indicate an increased static disorder for the smaller particles, but, less influenced thermal vibrations. For supported silver particles of 1.3 nm size an even larger increase of Debye–Waller factor was found and an Einstein temperature of 114 K [8]. The reduction of Einstein temperature of the samples investigated here follows the small effect seen in our data. This indicates surface specific increased vibrations at the particle–glass interface of the Ag containing glasses. This effect should be investigated further for silver particles incorporated into the glass network under various conditions. The drastic increase of the Debye–Waller factor for Ag-doped silicate glasses irradiated with low mass ions like He^+ or Li^+ should attributed to the static disorder [33] because the irradiation was performed at low temperatures through where no structural relaxation can be expected.

5.3. Third cumulant and thermal expansion

The third cumulant, C_3, reflects anharmonic vibrations of small silver particles. An asymmetric structural disorder at 10 K is neglected for bulk silver as reference material. Previous experiments on supported Ag particles of 1.3 nm size found a drastic trend to increase the thermal expansion coefficient (6.5 times) compared with the bulk fcc lattice [8]. The thermal expansion of the silver particles incorporated into a silicate glass is given in table 1. The parameters were calculated by equation (5). These values indicate the expected increase, e.g. by 20% for 2.5 nm particles, with decreasing particle size. However, the enlargement seems to be reduced for particles within a glass matrix because of distinctly different effects for isolated particles of 1.3 nm in size (75% of surface atoms) compared with embedded particles of 2.5 nm in size (50% of surface atoms). These drastic differences of more than one order of magnitude in the thermal expansion of particles quite similar in size are not expected by the role of the surface. Embedded and free particles also exhibit a very different behaviour of the Debye–Waller factor. Obviously, the existence of bonds across the particle–glass interface (e.g., Ag–O) is responsible for the observed changes in thermal expansion.

In general, the thermal expansion plays an important role for the stress state of small particles in composite materials. Here, silver particles are formed at elevated temperatures followed by a cooling procedure to room temperature. This procedure induces hydrostatic pressure if the thermal expansion of matrix and particle differs from each other and if these stresses cannot be relaxed. The thermal expansion of the investigated glass matrix at room temperature is 8×10^{-6} K^{-1}, i.e. much less than that of silver metals. Thus, a stress is expected within the nanoscale silver particles that has to be considered with respect to the atomic structure, i.e. concerning the lattice parameters, and with respect to the macroscopic properties, respectively.

Effects of the stress state on the structure of particles like dilatation or reduction of lattice parameters are well known (see next section). However, the influences of stress on the coefficient of thermal expansion were not investigated up to now although such experiments would be interesting. From a theoretical point of view only small effects are expected.

5.4. Ag–Ag bond length

Figure 6 represents the Ag–Ag distance of small particles determined by EXAFS experiments in comparison with experimental and thermodynamical values of the Ag bulk lattice. At 50 K, the EXAFS data of particles are similar to Ag foil values (2.5 nm particles) or slightly increased (6 nm particles). That means the typical lattice contraction of small particles is not observed in these glasses. High resolution electron microscopical investigations on similar glass samples confirm this effect [28]. These data demonstrate a lattice dilatation of 0.001 nm for small silver particles (3–6 nm in size) after cooling procedures as investigated here. The likely explanation of this expansion, neglecting any deviations from the Ag fcc lattice, is the interaction with the glass matrix. As mentioned before, a stress state, i.e. a tensile stress, within the silver particles can be induced during the cooling procedure after the formation of silver particles at elevated temperatures due to the low thermal expansion coefficient of the silicate glass compared with that of bulk silver or silver particles. Assuming the calculated parameters (see table 1), one would expect a stronger dilatation of 2.5 nm particles than for 6 nm ones for the same thermal treatment of both glasses that was, though, not observed. However, the starting temperature of glass I was 580 °C and for glass II 480 °C, respectively. With that, an increased temperature interval of 555 K for cooling to room temperature is responsible for stress generation for glass I compared with an interval of 455 K for glass II. Furthermore, relaxations of the glass

structure should be considered. The calculations of stresses by means of thermal expansion coefficients yield the maximum of the dilatation only. The exact description of generation of stress states in such composite materials would require a viscoelastic theory taken into account all thermoviscoelastic parameters of the soda-lime glass used. Such theory would also yield higher-order moments of the Ag–Ag pair distribution function evaluated in our experiments by EXAFS (see previous sections).

The evaluation of the thermal expansion by means of the Ag–Ag bond length $r(T)$ with temperature determined from the EXAFS phase currently does not provide the required precision (see the discussion in section 3). In contrast to the results of the more precise anharmonic Einstein model given above, the dependence of the Ag–Ag bond length on temperature shown in figure 6 would indicate a reduced thermal expansion of particles. Recently, Stern [15] and other authors [36, 37] proposed that small differences in interatomic distances determined by x-ray diffraction and EXAFS data originate from mean-squared vibrational disorder perpendicular to the line between the average position of the observed pair of atoms, $\sigma_\perp$ (here, the Ag–Ag pair). That leads to an additional contribution to the first cumulant, i.e. distance between two neighbouring atoms, determined by EXAFS. This part of the Debye–Waller factor causes a shift of the bond parameters for Ag foil and the silver particles. In the case of small particles, this effect should be reduced for atoms at the surface of the particle due to the lack of neighbouring silver atoms outside the particles, i.e. the interaction in one direction. For that reason, we expect a smaller correction of bond parameters of small particles at low temperatures, especially, for the smallest particles of 2.5 nm in size as well as a modified temperature dependence as a result of a specific dependence of the mean squared vibrational disorder perpendicular to the observed bond line. Considering this effect the correct Ag–Ag distances calculated from EXAFS experiments would show a stronger increase with increasing temperature in the range between 50 and 300 K that was investigated here. Consequently, the thermal expansion coefficient estimated on the basis of Ag–Ag distances would be increased compared with bulk material similar to that obtained by using anharmonicity parameters (see section 5.3). If the extended temperature interval for cooling of glass I is considered, in addition, the dependence of the lattice parameters of Ag particles determined by EXAFS data can be qualitatively explained within the complete range of temperatures investigated here. The confirmation of this model demands the calculation of the vibration modes within the surface of small particles and the introduction of these results into the evaluation of EXAFS data.

6. Conclusions

X-ray absorption experiments demonstrated that the Ag–Ag coordination shells of small silver particles as well as the oxygen environment of silver ions isolated within the glass matrix can be simultaneously characterized. Based on model assumptions, the fraction of both silver species is available.

In the case of embedded silver particles of 2.5 and 6 nm in size which are formed within the glass network by an ion exchange and subsequent thermal treatment, the structural parameters could be evaluated on the basis of temperature-dependent x-ray absorption experiments in the low-temperature range. It was found that the small silver particles show an unusual increase of lattice parameters compared with the silver foil and with isolated Ag particles because for nanoscale particles a contraction of the lattice is expected. This effect is most likely caused by the cooling process to room temperature subsequent to the formation of particles at elevated temperatures and due to the mismatch of thermal expansion coefficients of silver and glass matrix, the latter one being more than a factor of two smaller. Data evaluation of Ag K-edge

spectra on the basis of an anharmonic Einstein model showed an increase of Debye–Waller factor as well as of the thermal expansion coefficient of particles of 2.5 nm in size compared with bulk silver material whereas the parameters of particles of 6 nm in size were slightly changed only. The present results indicate that the dependence of the specific parameters on the size of the particles is less pronounced for embedded particles than for isolated or supported particles. This should be due to interactions between the metal particle and the surrounding glass matrix across the corresponding interface.

The structural investigations of silver particles embedded in a glass matrix reveal that the stress state of small inclusions in composite materials is determined by specific parameters of particles, by the nature of the interface and by the preparation procedure. It could be demonstrated that the lattice parameter of small particles determined by EXAFS spectroscopy represents a sensitive proof for all these processes.

Acknowledgment

This work has been supported by Deutsche Forschungsgemeinschaft (SFB 418).

References

[1] Hacke F, Ricard D and Flytzanis C 1986 *J. Opt. Soc. Am.* B **3** 1647
[2] Flytzanis C, Hache F, Klein M C, Ricard D and Rossignol Ph 1991 *Progress in Optics* vol XXIX, ed E Wolf (Amsterdam: Elsevier) p 322
[3] Monot R 1984 *Proc. Int. Symp. on the Physics of Latent Image Formation in Silver Halides (Trieste, 1983)* ed A Balderesci *et al* (Singapore: World Scientific) p 175
[4] Meiwes-Broer K H and Lutz H O 1991 *Physik. Bätter.* **47** 283
[5] Saka H, Nishikawa Y and Imura T 1988 *Phil. Mag.* **57** 895
[6] Giorgio S and Urban J 1988 *J. Phys. F: Met. Phys.* **18** 147
[7] Rockenberger J, Tröger L, Kornowski A, Vossmeyer T, Eychmüller A, Feldhaus J and Weller H 1997 *J. Phys. Chem.* B **101** 2691–701
[8] Yokoyama T, Kimoto S and Ohta T 1989 *Japan. J. Appl. Phys.* **28** 851
[9] Yokoyama T, Satsukawa T and Ohta T 1989 *Japan. J. Appl. Phys.* **28** 1905
[10] Wenzel L, Arvanitis D, Rabus H, Lederer T and Baberschke K 1990 *Phys. Rev. Lett.* **64** 1765
[11] Kuroda H, Yokoyama T, Asakura K and Iwasawa Y 1991 *Faraday Discuss. Chem. Soc.* **92**
[12] Arvanitis D, Lederer T, Comelli G, Tischer M, Yokoyama T, Tröger L and Baberschke K 1993 *Japan. J. Appl. Phys.* **32** (Supplement 32-2) 337
[13] Frenkel A I and Rehr J J 1993 *Phys. Rev.* B **48** 585
[14] Tröger L, Yokoyama T, Arvanitis D, Lederer T, Tischer M and Baberschke K 1994 *Phys. Rev.* B **49** 888
[15] Stern E A 1997 *J. Physique Coll.* VI **7** C2-137
[16] Berg K-J, Berger A and Hofmeister H 1991 *Z. Phys.* D **20** 313
[17] Dubiel M and Mosel G 1994 *Japan. J. Appl. Phys.* **33** 5892
[18] d'Acapito F, Gonella F, Cattaruzza E, Pascarelli S, Mazzoldi P and Mobilio S 1996 *Nucl. Instrum. Methods* B **120** 110
[19] Dubiel M, Brunsch S, Schwieger W and Brenn U 1998 *Proc. XVIIth Int. Congress on Glass* (San Francisco)
[20] Ankudinov A L 1996 *PhD Thesis* University of Washington
[21] Stern E A, Newville M, Ravel B, Yacoby Y and Haskel D 1995 *Physica* B **208/209** 117
[22] Tranquada J M and Ingalls R 1983 *Phys. Rev.* B **28** 3520
[23] Sandstrom D R, Marques E C, Biebesheimer V A, Lytle F W and Greegor R B 1985 *Phys. Rev.* B **32** 3541
[24] Bunker G 1983 *Nucl. Instrum. Methods* **207** 437
[25] Lee P A, Citrin P H, Eisenberger P and Kincaid B M 1981 *Rev. Mod. Phys.* **53** 769
[26] Zabinsky S I, Rehr J J, Ankudinov A L, Albers R C and Eller M J 1995 *Phys. Rev.* B **52** 2995
[27] Rabus H 1991 *PhD Thesis* Freie Universität, Berlin, p 120
[28] Dubiel M, Brunsch S, Mohr C and Hofmeister H 1998 *Proc. XVIIth Int. Congress on Glass* (San Francisco)
[29] K-H Hellwege (ed) 1981 *Landolt-Börnstein New Series Group III* vol 13 (Berlin: Springer)

[30] Touloukian Y S, Kirby R K, Taylor R E and Desai P D 1975 *Thermophysical Properties of Matter* vol 12 (New York: Plenum) p 298
[31] Dubiel M, Brunsch S, Kolb U, Gutwerk D and Bertagnolli H 1997 *J. Non-Cryst. Solids* **220** 30
[32] Houde-Walter S N, Inman J M, Dent A J and Greaves G N 1993 *J. Phys. Chem.* **97** 9330
[33] d'Acapito F, Gonella F, Cattaruzza E, Pascarelli S, Mazzoldi P and Mobilio S 1996 *Nucl. Instrum. Methods Phys. Res.* B **120** 110
[34] Fritsche H-G and Benfield R E 1993 *Z. Phys.* D **26** 15
[35] Tröger L, Hünnefeld H, Nunes S, Oehring M and Fritsch D 1997 *J. Phys. Chem.* B **101** 1279
[36] Dalba G, Fornasini P, Gotter R and Rocca F 1995 *Phys. Rev.* B **52** 149
[37] Dalba G, Fornasini P, Grisenti R, Pasqualini D, Diop D and Monti F 1998 *Phys. Rev.* B **58** 4793